Opt Quant Electron
DOI 10.1007/s11082-015-0189-z

Numerical modeling of long sub-wavelength patterned structures

Nadège Rassem[1] · Evgeny Popov[1] · Anne-Laure Fehrembach[1]

Received: 8 December 2014 / Accepted: 6 May 2015

Abstract The modeling of Cavity Resonator Integrated Grating Filter (CRIGF) structures, which are long but finite sub wavelength-patterned structures composed with a grating in-out coupler flanked with two Bragg reflectors, is challenging for any numerical method. We show how a numerical code based on RCWA, usually dedicated to model periodic structures, can be used, with minor modifications, to model CRIGFs within a reasonable time of calculation with a personal computer. Our results are in agreement with the calculations based on the FDTD method published in the literature.

Keywords Numerical method · Rigorous coupled waves analysis · Fourier modal method · grating · Bragg reflector

1 Introduction

Recently, a new promising optical component, known as Cavity Resonator Integrated Grating Filter (CRIGF) has been presented in the literature (Kintaka et al. 2010, 2012b; Inoue et al. 2014; Buet et al. 2012). It is composed of an in/out grating coupler (or Guided Mode Resonant Filter, GMRF), with a length of some tens of wavelengths, surrounded by two Bragg reflectors, each with a length of around one hundred of wavelengths, engraved on a waveguide layer (see Fig. 1a). The main interest of such a component is that it exhibits

✉ Anne-Laure Fehrembach
anne-laure.fehrembach@fresnel.fr

Nadège Rassem
nadege.rassem@fresnel.fr

Evgeny Popov
e.popov@fresnel.fr

[1] Aix-Marseille Université, CNRS, Centrale Marseille, Institut Fresnel UMR 7249, 13013 Marseille, France

Published online: 27 May 2015

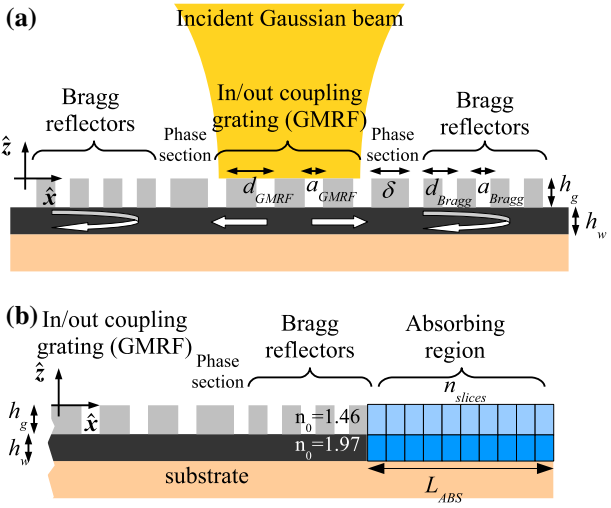

Fig. 1 **a** Definition of the notations for the parameters of the structure. **b** Representation of the absorbing region on the right hand side of the structure

mode resonances with a low spectral bandwidth (below 1 nm in the optical range) and a wide angular acceptance (several degrees), one order of magnitude greater than that of simple GMRFs which are known for their low angular acceptance (Fehrembach et al. 2010). The extra-ordinary wide angular acceptance of CRIGFs as compared to simple GMRFs may be incomprehensible at a first sight, since one can consider that in simple GMRFs, the second harmonic of the grating acts as a Bragg grating (Avrutskii et al. 1986). Yet even with complex basic patterns designed to enhance the second harmonic of the grating (Fehrembach et al. 2010), the angular acceptance of GMRFs is $<1°$. To go further, it is interesting to compare the properties of infinite gratings composed with a grating coupler and a Bragg grating one above the other (Lemarchand et al. 1998) (infinite grating) with that of CRIGFs (grating coupler and Bragg grating one beside the other). This comparison, together with a physical explanation of the extra-ordinary wide angular acceptance of CRIGFs are given in Rassem et al. (2015). Thus CRIGFs are promising components and being able to numerically model them is crucial.

Yet, the length of the structure and its sub-wavelength patterning makes it difficult to model numerically. In the previous works, the design of the components where done using an approximate model based on the Coupled Mode Theory (Ura et al. 2011), or rigorous calculations with the Finite Difference Time Domain (FDTD) method (Buet et al. 2012; Kintaka et al. 2012a). Among the numerical methods that could be used to model CRIGFs [Finite Element Method (Demésy et al. 2014), Coupled Dipole Method (Chaumet et al. 2003), Rigorous Coupled Wave Analysis...] only results based on the FDTD method have been published.

The aim of this paper is to show that modeling CRIGFs with the Rigorous Coupled Wave Analysis (also known as Fourier Modal Method) is possible within a reasonable time of calculation, and to identify a set of correct convergence parameters. In the following, we recall the basic principles of RCWA and present how we adapt it to the modeling of CRIGFs. We show the results of the tests of convergence of our numerical code and apply it to the study of the behaviour of CRIGFs with respect to the incidence parameters.

2 Basic principles of the modeling of CRIGFs with RCWA

RCWA is a well known theory for modeling structures which are periodic along two directions (say x and y), with a staircase variation of the permittivity in the third direction (z) (Moharam and Gaylord 1983; Bruer and Bryngdahl 1993; Noponen and Turunen 1994). As the structure is periodic, the permittivity function is expanded as a Fourier series and the electromagnetic field is expanded as a Floquet-Bloch series, which turns into a Rayleigh series in homogeneous regions. In a region with a grating, a differential equation can be derived from Maxwell equations that relates the tangential electric and magnetic components of the field to their derivative with respect to z:

$$\frac{\mathrm{d}\mathbf{F}}{\mathrm{dz}} = \mathbf{MF}, \tag{1}$$

where the tangential electric and magnetic components of the Floquet-Bloch coefficients of the field are gathered in the column vector $\mathbf{F}$. The $\mathbf{M}$ matrix depends on the Fourier coefficients of the grating, the wavelengh and the in-plane (x–y) components of the wavevector of the diffraction orders. The size of the $\mathbf{M}$ matrix is proportional to the order N of truncation of the series. If the permittivity of the grating depends on z, it is possible to numerically integrate Eq. 1 (see the literature on the differential method Popov 2014). For z-independent grating shapes, Eq. 1 is solved by calculating the eigenvalues and eigenvectors of the $\mathbf{M}$ matrix, which correspond to the modes propagating in a structure with the same permittivity as the grating, but infinite in the z direction.

A large amount of work has been performed to improve the speed of convergence of the RCWA, especially through a correct implementation of the factorization of the product of Fourier series (Li 1996a, 1997). Moreover, the numerical stability of the method can benefit from the use of the S-matrix algorithm or one of its variant (Li 2003, 1996b). From now on, the RCWA method shows no convergence nor numerical stability problems for structures composed with dielectric materials or metals with in the visible spectrum (Li 2014). The most time-consuming operation is the calculation of the eigenvalues and eigenvectors of the $\mathbf{M}$ matrix, which grows with the number $(2N + 1)$ of Fourier coefficients. All the calculations presented in this paper are done with a home-made numerical code based on RCWA improved with the S-matrix algorithm (Li 2003) and the correct implementation of the rules of factorization of the product of Fourier series (Li 1997).

CRIGFs are structures which contains sub-wavelength pattern, over hundred of wavelengths long but finite areas (see Fig. 1a). In order to model a CRIGF with our RCWA code made to model periodic structures, we use the so-called "super-cell" method, which consists in considering the CRIGF as the basic pattern of a grating. For the modeling to be valid, it is necessary to isolate each basic cell from its neighbours. For this reason, we add an absorbing region between each basic cell, as was first suggested in Silberstein et al. (2001) (see Fig. 1b). This method is now known as a-RCWA (for aperiodic-RCWA) (see for example Maes et al. 2013). Our absorbing region consists of n_{slices} homogeneous rectangular rods for a total thickness L_{ABS} (see Fig. 1b). The refractive index n_p of the p^{th} rod is $n_p = n_0 + i[p/n_{slices}]^2$, where p is an integer varying from 1 to n_{slices} and n_0 is the index of the material of the layer of the structure immediately adjacent to the absorbing region. The absorbing region can be added inside the grating and waveguide regions. Note that it is not necessary to insert an absorbing region inside the substrate and superstrate as long as we are interested in the energy

reflected and transmitted by the structure. Indeed, RCWA allows to calculate directly the coefficients of the Rayleigh expansion of the field in the substrate and superstrate, and the reflected and transmitted energy are calculated from these coefficients. This is different from other methods such as Finite Element Method or Finite Difference Time Domain method which calculate first the field and then the coefficients of the Rayleigh expansion of the field. Considering an infinity of basic patterns to model only one pattern can lead problems in the diffracted field because of the interferences which occur between the field coming from the different basic patterns, and inserting absorbing regions inside the substrate and superstrate would be necessary in this case.

From a numerical point of view, CRIGF is modeled as a grating with a period equals to several hundred of wavelengths, which means that several hundred propagative orders of diffraction exist. Our numerical code calculates the scattering **S**-matrix of the structure that relates the field in the diffraction orders to the incident ones. The incident field is a Gaussian beam, expanded on a plane wave basis. In order to reduce the calculation time, we expand the Gaussian beam over the diffraction orders of the grating, thus requiring only one calculation of the **S**-matrix for each wavelength. The energy of the incident beam is set to unity, and we calculate the energy reflected in the specular beam by summing the energy reflected in the same diffraction orders as those used to illuminate the component.

3 Convergence and validation of the numerical code

The aim of this section is to show how we can efficiently model 1D-CRIGFs with the RCWA. For all the calculations, the parameters of the structure considered are (see Fig. 1): $h_w = 165, h_g = 120, d_{GMRF} = 529.43, a_{GMRF} = 99.5, d_{Bragg} = 266, a_{Bragg} = 100$ nm, $n_{GMRF} = 21, n_{Bragg} = 200$, $\delta = d_{GMRF}$. The grating is engraved in a layer of SiO_2, with refractive

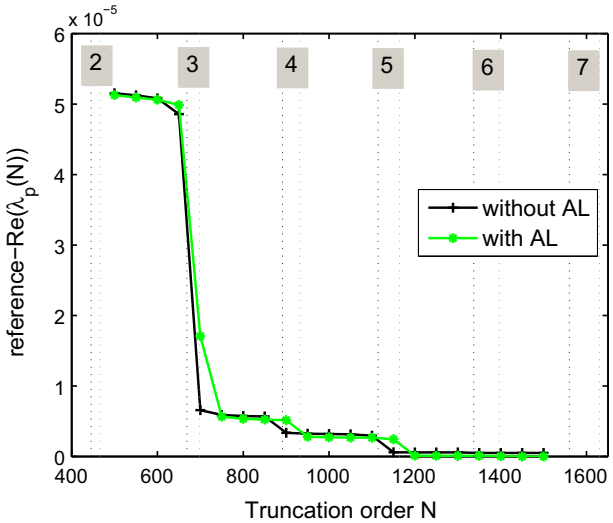

Fig. 2 Convergence of the numerical code with respect to the truncation order N, without (*black crosses*) and with (*green stars*) absorbing layers. "reference" correspond to the real part of the wavelength pole λ_p for $N = 1500$ with absorbing layers

index 1.46 (the holes are filled with air), the guiding layer has a refractive index of 1.97, and the substrate is also SiO_2. The parameters are quite the same as that of the structure presented in Buet et al. (2012) except that only the top layer is engraved and that we have modified the GMRF period to shift the resonance peak toward the center of the Bragg band-gap. We calculated the edges of the band-gap of the (infinite along x) Bragg grating (861.6 and 872.8 nm) using our numerical code based on RCWA.

3.1 Convergence with respect to the number of Fourier coefficients

As often when dealing with resonant structures, the centering wavelength of the resonance is one of the characteristic most sensitive to the truncation order. We have calculated the wavelength of the mode that can be excited under normal incidence, i.e., the wavelength pole λ_p of the determinant of the scattering matrix in the zero diffraction order, for increasing values of the truncation order N. The resonance peak is expected to occur at a wavelength close to the real part of λ_p [Re(λ_p)].

We show in Fig. 2 the real part of λ_p for a truncation order N varying from 500 to 1500 by step of 50 ($2N+1$ Fourier coefficients), with absorbing regions ($n_{slices} = 10, L_{ABS} = 2.66\,\mu$m) and without. We observe that the convergence rate with respect to N has a staircase behaviour. This can be explained by the fact that the excitation of the mode through the coupling grating (GMRF) occurs when the in-plane wave vector of one diffraction order of the GMRF matches that of the mode. In our case, the coupling grating was designed to couple the mode through its first diffraction order, and the total length $L = 117{,}980$ µm is around 222 times greater than d_{GMRF} without absorbing region, and with absorbing regions $L = 123{,}275$ µm is around 232 times greater than d_{GMRF}. We have represented in Fig. 2 with black (case without absorbing regions) and green (case with absorbing regions) vertical lines the limits corresponding to the second, third, fourth, ... seventh diffraction orders of the GMRF. The integers indicated in the gray boxes on the top of the graph correspond to the floor integer part of $N/(L/d_{GMRF})$ for each case (with and without absorbing region). The steps of the staircases occur when a supplementary order of diffraction of the GMRF is taken into account in the modeling. We observe that a truncation order of 700 without absorbing region leads to results with a good precision, which is reached with $N = 750$ with absorbing regions, and that the two modeling converge to

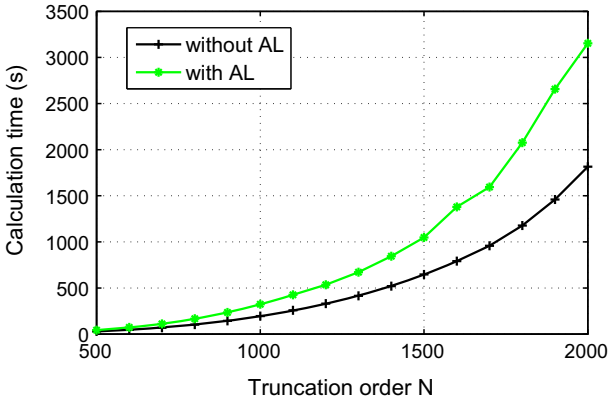

Fig. 3 Calculation time of the reflectivity with respect to the truncation order (job dispatched over 8 threads on a personal computer with a bi-processors with 8 cores at 3.10 GHz)

values very close to each other. This means that the benefit of introducing absorbing regions is negligible, and this is true because the range of wavelengths considered is well inside the band-gap of the Bragg grating.

We plotted in Fig. 3 the calculation time versus N for a single calculation of the reflectivity, using 8 threads on a personal computer with a bi-processors with 8 cores at 3.10 GHz. A calculation with $N = 800$ takes around 102 s per point without absorbing region and 167 s per point with absorbing region. The calculation time is greater when absorbing regions are added because in this case, each layer (even the homogeneous ones) is modeled as a non-homogeneous layer, thus requiring the resolution of the eigen problem associated with the **M** matrix of the layer (see Eq. 1).

In order to check the convergence of the width and maximum value of the peak with respect to the truncation order, we plot in Fig. 4 the spectra for several values of the truncation order, with and without absorbing region. We observe that the maximum value of the peak and its width remain similar for the various values of N. The maximum of the peak is higher without absorbing regions than with absorbing regions (around 0.784 with absorbing region versus 0.788 without). This is due to the fact that the remaining part of the guided mode that is not reflected by the Bragg mirror is lost inside the absorbing regions. The spectral width of the peak at half maximum is around 0.36 nm with and without absorbing regions.

For wavelengths lying outside the gap, it is important to model the finite component with absorbing regions included between each basic cell. To illustrate this, we plotted in Fig. 5 the spectra obtained outside the band gap for $N = 900$. We observe a sharp peak in the spectrum modeled without absorbing region that disappears in the spectrum modeled with absorbing region. Inside the band-gap (for wavelengths smaller than the superior edge of the gap which is indicated with the vertical blue dotted line), the two curves are superimposed.

From this study, we conclude that using absorbing regions is important especially for wavelengths outside the band-gap of the Bragg grating and that a truncation order of 800 leads to a good precision, with a reasonable computation time of 167 s per point for one wavelength.

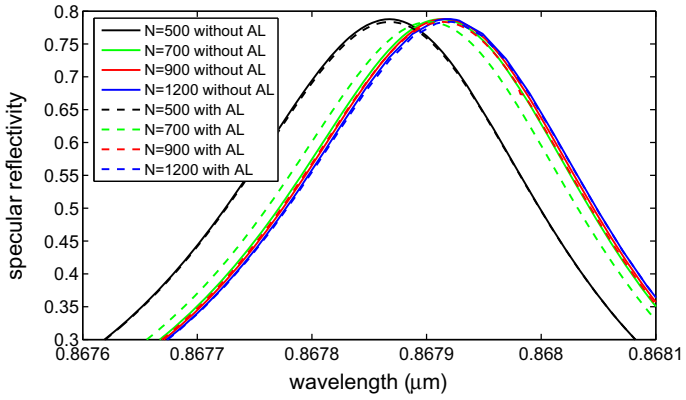

Fig. 4 Reflectivity spectra for varying values of the truncation order N, with absorbing regions (*solid line*) and without (*dotted line*)

3.2 Comparison with results from the literature

In order to validate our results, we consider the structure described in Buet et al. (2012) for which the spectrum was calculated using FDTD (see Fig. 2a of Buet et al. 2012). We plot in Fig. 6 the spectrum calculated with our numerical code with absorbing layers ($L_{abs} = 2.66$ µm and $n_{slices} = 10$) and truncation order $N = 950$ for a beam waist radius of 5.71 µm for which the maximum of the peak is maximum. We observe a spectrum which is similar to that in Buet et al. (2012). The peak reaches 0.882 at its maximum and its width at half maximum is 0.6 nm, in agreement with the values obtained in Buet et al. (2012). It is centered at 861.4 nm, against 858 nm in Buet et al. (2012). The slight difference between the centering wavelength may be explained in part by the fact that the pattern is discretized when modeled with FDTD while the Fourier coefficients are calculated analytically in our numerical code.

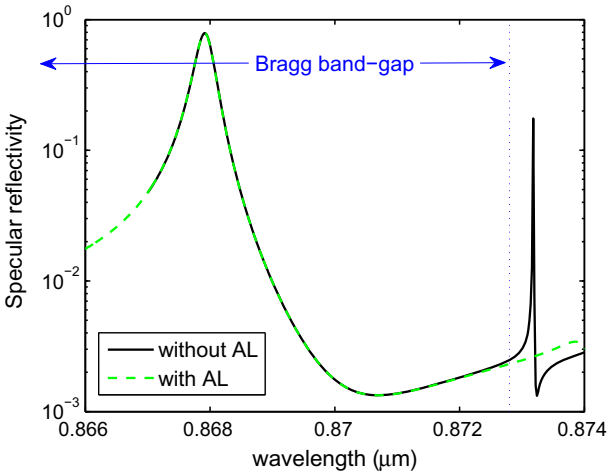

Fig. 5 Reflectivity spectra outside the band-gap of the Bragg grating without absorbing region (*black solid line*) and with (*green dotted line*). The superior edge of the gap is indicated with the *vertical dotted blue line*

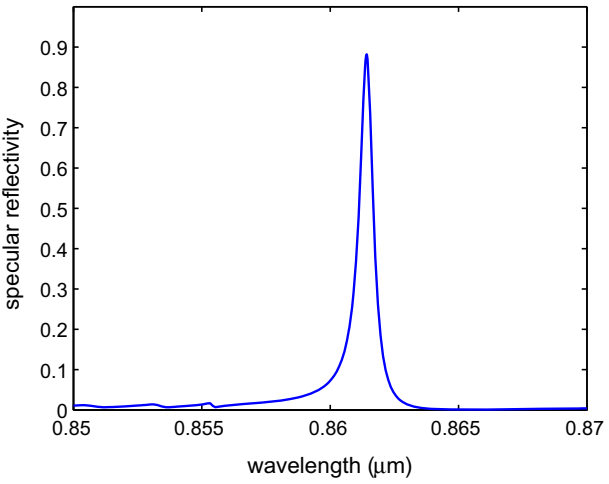

Fig. 6 Reflectivity spectrum of the structure of Buet et al. (2012) calculated with our numerical code

4 Modification of the incident beam

In this section, we illustrate the use of the RCWA to analyse the properties of the CRIGF with respect to the incidence beam. The parameters of the structure are the same as in the Sect. 3.1. In the modeling, we used a truncation order $N = 950$, with absorbing region having a thickness $L_{ABS} = 2.66\,\mu$m and $n_{slices} = 10$. Below, we show the effect of modifying the waist radius of the incident beam and its central angle of incidence. Let us emphasize that because of the numerous diffraction orders of the modeled structure, only one calculation of the scattering matrix per wavelength is necessary when varying the waist radius and the angle of incidence. Hence, the calculation for several angles of incidence and several waists takes almost the same time as for only a single set.

4.1 Variation of the beam waist

We plot in Fig. 7a the reflected energy (taking into account all the diffraction orders, and not only the specular beam) versus the beam waist radius (normalized with respect to the width of the GMRF) and the wavelength. We observe that the reflectivity is maximal for a beam waist to GMRF width ratio close to 0.5. The reflectivity decreases for smaller waists because the divergence of the beam is greater than the angular acceptance of the mode. The reflectivity decreases for greater waists because the incident beam spreads over the Bragg grating, and this part of the beam which does not couple to the GMRF mode is transmitted. This is confirmed in Fig. 7b representing the reflected, transmitted and absorbed (in the absorbing regions) energy for a wavelength equal to 867.9 nm (for which the reflectivity is maximum). Almost all the energy that is not reflected is transmitted. The absorption remains very low (around 10^{-3}) and is maximal when the reflectivity is maximal, in agreement with the fact that the reflectivity peak is due to the excitation of a mode that extends inside the waveguide layer. The behavior of the reflectivity with respect to the beam waist radius confirms the measures reported in Buet et al. (2012).

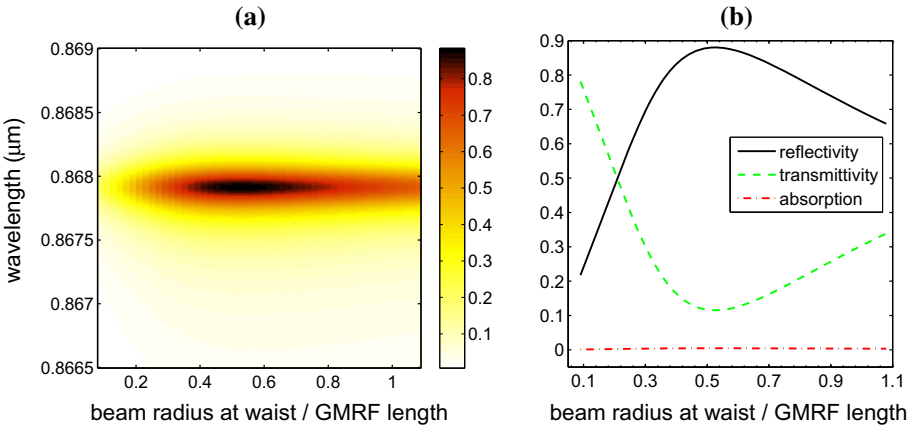

Fig. 7 **a** Reflectivity versus the radius of the incident beam at waist (normalized with respect to the GMRF width) and the wavelength λ. **b** Reflectivity (*black solid line*), transmittivity (*green dashed line*) absorption (*red dash-dotted line*) with respect to the radius of the incident beam at waist (normalized with respect to the GMRF width) for 867.9 nm

4.2 Variation of the angle of incidence

We plot in Fig. 8 the reflectivity versus the angle of incidence and the wavelength. We observe a maximum of reflectivity for wavelength around 867.9 nm, which spreads from $-2°$ to $2°$, thus confirming the wide angular acceptance of CRIGFs. This plot emphasizes the different behaviors of CRIGFs and the classical (infinite) GMRFs with respect to the angle of incidence. In particular for GMRFs, the reflectivity versus the angle of incidence and the wavelength shows an upper and a lower branch at each side of a bang-gap (Rassem et al. 2015).

5 Conclusion

To model a CRIGF with our numerical code based on RCWA, we considered it as the basic cell of a periodic pattern and added absorbing regions between each basic cell. We showed that CRIGFs are well adapted to the super cell method since the mode is almost entirely reflected back inside the Bragg reflector thus the absorbing regions are not essential for wavelengths lying inside the Bragg band-gap, which case is the range of interest in the studies of CRIGFs. A reasonable time of calculation is reached thanks to the good rate of convergence of RCWA for dielectric gratings, and also because we benefit from the expansion of the Gaussian beam over the numerous diffraction orders of the modeled component. Our results confirm those obtained with the FDTD method published in the literature.

As an application of this work we are now studying the dependence of the CRIGF spectral properties with respect to its physical parameters, in order to identify the role of each parameter. Further improvement of our numerical code could use the fact that the CRIGF is composed with patterns which are almost periodic (the grating coupler and the Bragg mirror) thus a large amount of the Fourier coefficients of the structure is negligible.

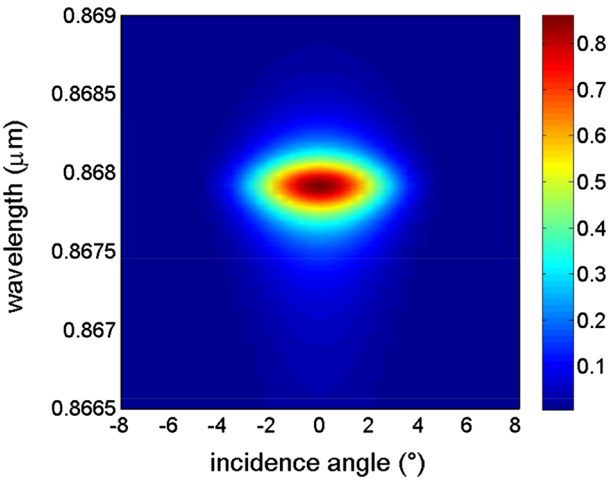

Fig. 8 Reflectivity in the specular beam (waist radius 5.24 μm) versus the angle of incidence θ and the wavelength λ

References

Avrutskii, I.A., Golubenko, G.A., Sychugov, V.A., Tishchenko, A.V.: Spectral and laser characteristics of a mirror with a corrugated waveguide on its surface. Sov. J. Quantum Electron. **16**, 1063–1065 (1986)

Bruer, R., Bryngdahl, O.: Electromagnetic diffraction analysis of two-dimensional gratings. Opt. Comm. **100**, 1–5 (1993)

Buet, X., Daran, E., Belharet, D., Lozes-Dupuy, F., Monmayrant, A., Gauthier-Lafaye, O.: High angular tolerance and reflectivity with narrow bandwidth cavity-resonator-integrated guided-mode resonance filter. Opt. Express **20**, 9322–9327 (2012)

Chaumet, P.C., Rahmani, A., Bryant, G.W.: Generalization of the coupled dipole method to periodic structures. Phys. Rev. B **67**, 165404 (2003)

Demésy, G., Zolla, F., Nicolet, A., Vial, B.: Finite element method. In: Popov, E. (ed.) Gratings: Theory and Numeric Applications, Second Revisited Edition, AMU (PUP), pp. 5.1–5.48 (2014), www.fresnel.fr/numerical-grating-book-2

Fehrembach, A.-L., Lemarchand, F., Talneau, A., Sentenac, A.: High Q polarization independent guided-mode resonance filter with doubly periodic etched Ta2O5 bidimensional grating I.E.E.E. J. Lightwave Technol. **28**, 2037–2044 (2010)

Inoue, J., Ogura, T., Kondo, T., Kintaka, K., Nishio, K., Awatsuji, Y., Ura, S.: Reflection characteristics of guided-mode resonance filter combined with bottom mirror. Opt. Lett. **39**, 1893 (2014)

Kintaka, K., Kita, Y., Shimizu, K., Matsuoka, H., Ura, S., Nishii, J.: Cavity-resonator-integrated grating input/output coupler for high-efficiency vertical coupling with a small aperture. Opt. Lett. **35**, 1989–1991 (2010)

Kintaka, K., Majima, T., Inoue, J., Hatanaka, K., Junji, N., Ura, S.: Cavity-resonator-integrated guided-mode resonance filter for aperture miniaturization. Opt. Express **20**, 1444–1449 (2012a)

Kintaka, K., Majima, T., Hatanaka, K., Inoue, J., Ura, S.: Polarization-independent guided-mode resonance filter with cross-integrated waveguide resonators. Opt. Lett. **37**, 3264–3266 (2012b)

Lemarchand, F., Sentenac, A., Giovannini, H.: Increasing the angular tolerance of resonant grating filters with doubly periodic structures. Opt. Lett. **23**, 1149–1151 (1998)

Li, L.: Fourier modal method In: Popov, E. (ed.) Gratings: Theory and Numeric Applications, Second Revisited Edition, AMU (PUP), pp. 13.1–13.40 (2014), www.fresnel.fr/numerical-grating-book-2

Li, L.: Use of Fourier series in the analysis of discontinuous periodic structures. J. Opt. Soc. Am. A **13**, 1870–1876 (1996a)

Li, L.: Formulation and comparison of two recursive matrix algorithms for modeling layered diffraction gratings. J. Opt. Soc. Am. A **13**, 1024–1033 (1996b)

Li, L.: New formulation of the Fourier modal method for crossed surface-relief gratings. J. Opt. Soc. Am. A **14**, 2758–2767 (1997)

Li, L.: Note on the S-matrix propagation algorithm Jo. Opt. Soc. Am. A **20**, 655–660 (2003)

Maes, B., Petracek, J., Burger, S., Kwiecien, P., Luksch, J., Richter, I.: Simulations of high-Q optical nanocavities with a gradual 1D bandgap. Opt. Express **21**, 6794–6806 (2013)

Moharam, M.G., Gaylord, T.: Three-dimensional vector coupled-wave analysis of planar-grating diffraction. J. Opt. Soc. Am. **73**, 1105–1112 (1983)

Noponen, E., Turunen, J.: Eigenmode method for electromagnetic synthesis of diffractive elements with three-dimensional profiles. J. Opt. Soc. Am. A **11**, 2494–2502 (1994)

Popov, E.: Differential method for periodic structures. In: Popov, E. (ed.) Gratings: Theory and Numeric Applications, Second Revisited Edition, AMU (PUP), pp. 7.1–7.57 (2014), www.fresnel.fr/numerical-grating-book-2

Rassem, N., Fehrembach, A.-L., Popov, E.: Waveguide mode in the box with an extraordinary flat dispersion curve. J. Opt. Soc. Am. A **32**, 420–430 (2015)

Silberstein, E., Lalanne, P., Hugonin, J.-P., Cao, Q.: Use of grating theories in integrated optics. J. Opt. Soc. Am. A **18**, 2865–2875 (2001)

Ura, S., Inoue, J., Kintaka, K., Awatsuji, Y.: Proposal of Small-Aperture Guided-Mode Resonance Filter ICTON 2011, Th.A4.4 (2011)